# Microwave-assisted switching of a nanomagnet: Analytical determination of the optimal microwave field

N. Barros, H. Rassam, and H. Kachkachi

*PROMES-CNRS and Université de Perpignan Via Domitia, 52 Avenue Paul Alduy, 66860 Perpignan Cedex, France*

(Received 18 March 2013; revised manuscript received 10 June 2013; published 19 July 2013)

We analytically determine the optimal microwave field that allows for the magnetization reversal of a nanomagnet modeled as a macrospin. This is done by minimizing the total injected energy. The results are in good agreement with the fields obtained numerically using the optimal control theory. For typical values of the damping parameter, a weak microwave field is sufficient to induce switching through a resonant process. The optimal field is orthogonal to the magnetization direction at any time and modulated in both amplitude and frequency. The dependence of the pulse shape on the applied field and damping parameter is interpreted. The total injected energy is found to be proportionnal to the energy barrier between the initial state and the saddle point and to the damping parameter. This result may be used as a means for probing the damping parameter in real nanoparticles.

DOI: 10.1103/PhysRevB.88.014421 PACS number(s): 75.10.Hk, 75.75.Jn, 84.40.−x

## I. INTRODUCTION

Magnetic recording is a key technology in the field of high density information storage. In order to increase thermal stability, small nanoparticles with high anisotropy may be used. However, high fields are then needed to reverse the magnetization but these are difficult to achieve in current devices. To overcome this so-called magnetic recording trilemma, several solutions are being proposed. The most investigated route, and the one that already leads to industrial applications, is the heat-assisted magnetic recording.[1] It consists of heating the particles by a laser which decreases the energy barrier between the two energy minima and thereby the switching fields. However, to avoid a loss of information, the heating must be very localized and followed by a very fast cooling, and as such these devices must be coupled to powerful heat dissipation systems.

An alternative solution is to assist the switching by a microwave (MW) field. In 2003 Thirion *et al*.[2] showed that the combination of a dc applied field (static field) well below the switching field with a small MW field pulse can reverse ;the magnetization of a nanoparticle. Indeed, in the presence of a MW field with appropriate amplitude and frequency, the magnetization precession synchronizes with this field.[3–5] Then, energy is pumped into the system thus allowing the magnetization to climb up the energy barrier and cross the saddle point.[6–10] Further experimental and theoretical studies have proven that this process is more efficient if the frequency of the MW field is sligthly lower than the ferromagnetic resonance frequency of the nanoelements.[11–13] Moreover, the use of chirped MW fields has been shown to be more efficient to achieve switching.[7,11,14–16] This result is related to the anharmonicity of the energy well. Similar results have been obtained in other areas of physics and chemistry, like atomic or molecular spectroscopy.[17,18]

In a previous work[19] we developed a numerical method based on optimal control theory which renders an exact solution for the MW field that is necessary for the switching of a nanomagnet within a given potential energy. The formulation of this method consists of defining a cost functional and minimizing it using the conjugate gradient technique. Our results confirmed that a weak MW field, modulated in both amplitude and frequency, can induce the switching of the magnetization. Furthermore, the injected energy was found to increase with damping.

The aim of the present study is to provide analytical expressions and to compare them with our numerical results by using simple energy considerations. Moreover, the analytical developments presented here confirm the effects observed numerically and provide clear interpretations for the underlying physical processes. In this work, our investigations are restricted to zero temperature, and as such the Landau-Lifshitz-Gilbert equation is used to describe the magnetization trajectory. The additional effects of thermal fluctuations will be the subject of a future study.

In the first part, we analytically determine the optimal MW field and demonstrate its dependence on the energy landscape (anisotropy, applied field) and on the damping parameter. We then investigate the trajectory of the magnetization in the presence of the optimal field and show that it can be described by the Landau-Lifshitz-Gilbert equation with a negative damping parameter. In the second part, the analytical results are compared directly with the results obtained numerically using the optimal control theory.

## II. ANALYTICAL CALCULATION OF THE OPTIMAL MICROWAVE FIELD

We consider a nanomagnet with spatially uniform magnetization which can be modeled by the vector $\mathbf{M} = M_S\mathbf{m}$, where $M_S$ is the saturation magnetization and $\|\mathbf{m}\| = 1$. This nanomagnet is characterized by a given anisotropy (uniaxial, biaxial, cubic...) and the damping parameter $\alpha$. In the presence of a static magnetic field, $\mathbf{H}_0$, lower than the Stoner-Wohlfarth switching field, the potential energy surface presents several minima separated by saddle points.

At the initial time $t_i$, we assume that the magnetization is in a minimum $\mathbf{M}_i = M_S\mathbf{m}_i$. Adding a microwave (MW) field, $\mathbf{H}(t)$, can then induce switching to another (target) minimum, $\mathbf{M}_f = M_S\mathbf{m}_f$. Our aim is to find the optimal field $\mathbf{H}^{\rm opt}(t)$ that achieves switching in a given time, $t_f$, while minimizing the energy injected into the system. This criterion is relevant

 

for experimental devices since it amounts to reducing both the intensity and the duration of the applied fields and the subsequent heating of the system, which can be of interest for magnetic recording or biomedical applications. This approach is thus complementary to other theoretical studies which have focused on the reduction of the switching time.[9,20]

For the sake of simplicity, we introduce the normalized fields $\mathbf{h}_0 \equiv \mathbf{H}_0/H_{\rm an}$ and $\mathbf{h}(t) \equiv \mathbf{H}(t)/H_{\rm an}$, where $H_{\rm an} \equiv 2K/\mu_0 M_s$ is the anisotropy field and $K$ the anisotropy constant of the nanomagnet. We also define the normalized time $\tau \equiv \gamma H_{\rm an} t$, where $\gamma = 1.76 \times 10^{11}$ ($\mathrm{T}^{-1}\,\mathrm{s}^{-1}$) is the gyromagnetic factor. For instance, for a cobalt particle of 3 nm in diameter with $K \approx 2.2 \times 10^5$ J m$^{-3}$ and $M_s \approx 1.44 \times 10^6$ A m$^{-1}$, we have $\mu_0\, H_{\rm an} \approx 305$ mT and $t/\tau \approx 1.86 \times 10^{-11}$ s.

### A. Energy and time trajectory in the presence of a microwave field

If only the static field is applied, the energy density of the system (divided by $2K$) reads $\mathcal{E}_0(\mathbf{m},\mathbf{h}_0) = \mathcal{E}_{\rm an}(\mathbf{m}) - \mathbf{m}\cdot\mathbf{h}_0$, where $\mathcal{E}_{\rm an}$ is the anisotropy energy density. The normalized effective field is then defined by $\mathbf{h}_{\rm eff} \equiv -\partial\mathcal{E}_0/\partial\mathbf{m}$. If we add a MW field, the energy density becomes

$$\mathcal{E}[\mathbf{m},\mathbf{h}_0,\mathbf{h}(\tau)] = \mathcal{E}_{\rm an}(\mathbf{m}) - \mathbf{m}\cdot[\mathbf{h}_0 + \mathbf{h}(\tau)] \tag{1}$$

and the normalized total effective field now reads

$$\boldsymbol{\zeta}(\tau) \equiv -\frac{\partial\mathcal{E}}{\partial\mathbf{m}} = \mathbf{h}_{\rm eff} + \mathbf{h}(\tau). \tag{2}$$

The time trajectory of the magnetization can be described by the driven Landau-Lifshitz-Gilbert equation:

$$(1+\alpha^2)\frac{d\mathbf{m}}{d\tau} = -\mathbf{m}\times\boldsymbol{\zeta}(\tau) - \alpha\mathbf{m}\times[\mathbf{m}\times\boldsymbol{\zeta}(\tau)]\,. \tag{3}$$

This allows us to express the energy variation of the system as follows

$$\begin{aligned}\frac{d\mathcal{E}}{d\tau} &= -\boldsymbol{\zeta}(\tau)\cdot\frac{d\mathbf{m}}{d\tau} - \mathbf{m}\cdot\frac{d\mathbf{h}(\tau)}{d\tau}\\ &= -\mathbf{h}_{\rm eff}\cdot\frac{d\mathbf{m}}{d\tau} - \frac{d}{d\tau}[\mathbf{m}\cdot\mathbf{h}(\tau)]\,.\end{aligned} \tag{4}$$

Next, we define the mobile frame $(\mathbf{m},\mathbf{u},\mathbf{v})$ attached to the magnetization with $\mathbf{u} \equiv \mathbf{T}/T$ and $\mathbf{v} \equiv \mathbf{m}\times\mathbf{T}/T$, where $\mathbf{T} \equiv \mathbf{m}\times\mathbf{h}_{\rm eff}$ and $T = \|\mathbf{m}\times\mathbf{h}_{\rm eff}\|$. The MW field can then be decomposed as $\mathbf{h}(\tau) = h_m(\tau)\mathbf{m} + h_u(\tau)\mathbf{u} + h_v(\tau)\mathbf{v}$. In this frame, Eqs. (3) and (4), respectively, become

$$\begin{aligned}(1+\alpha^2)\frac{d\mathbf{m}}{d\tau} &= \left(-1 + \frac{\alpha\, h_u(\tau) + h_v(\tau)}{T}\right)\mathbf{T}\\ &\quad - \left(\alpha + \frac{h_u(\tau) - \alpha h_v(\tau)}{T}\right)(\mathbf{m}\times\mathbf{T}),\end{aligned} \tag{5}$$

$$\frac{d\mathcal{E}}{d\tau} = \frac{-\alpha T - h_u(\tau) + \alpha h_v(\tau)}{1+\alpha^2}\,T - \frac{dh_m(\tau)}{d\tau}. \tag{6}$$

We note that the parallel component of the MW field, $h_m(\tau)$, has no direct effect on the magnetization trajectory and that only its time derivative appears in the energy variation.

### B. Optimization of the MW field

In order to find the optimal MW field fulfilling the requirements described earlier we proceed in two steps. First, we define the critical MW field which allows us to maintain the precession of the magnetization by compensating the effects of damping (Sec. II B 1). This field represents the lower limit for the optimal field sought. Using this result, we find the optimal MW field minimizing the injected energy (Sec. II B 2) and check that it can induce switching of the magnetization (Sec. II B 3).

#### *1. MW field maintaining the precession: Critical field*

In order to induce switching the MW field must at least compensate for the effect of damping, which tends to take the magnetization back to the initial equilibrium position. If the compensation is complete the energy variation of the system, $d\mathcal{E}/dt$, vanishes at any time, thus reflecting the conservation of energy. According to Eq. (6) an infinity of MW fields leads to a full compensation of damping. For instance, any field that is orthogonal to the magnetization so that $h_m(\tau) = 0$ and satisfying the equation $-h_u(\tau) + \alpha h_v(\tau) = -\alpha T$ will do.

Among these MW fields the critical field can be defined as the one that minimizes the power injected in the system. The latter is proportional to the squared intensity of the MW field, i.e., $p_i(\tau) = \mathbf{h}^2(\tau) = h_m^2(\tau) + h_u^2(\tau) + h_v^2(\tau)$. Using the method of Lagrange multipliers we define the functional

$$L\,[h_m(\tau), h_u(\tau), h_v(\tau), \lambda(\tau)] = p_i^2(\tau) - \lambda(\tau)\frac{d\mathcal{E}}{d\tau}. \tag{7}$$

Assuming that $dh_m(\tau)/d\tau$ does not depend explicitly on $h_m(\tau)$, the minimization of this functional leads to

$$h_m(\tau) = 0, \quad h_u(\tau) = -\frac{\alpha}{1+\alpha^2}\,T, \quad h_v(\tau) = \frac{\alpha^2}{1+\alpha^2}\,T. \tag{8}$$

The critical MW field thus reads

$$\mathbf{h}^{\rm crit}(\tau) = \frac{\alpha}{1+\alpha^2}\,[-\mathbf{T} + \alpha\,\mathbf{m}\times\mathbf{T}] \tag{9}$$

and the injected power is then

$$p_i^{\rm crit}(\tau) = \frac{\alpha^2}{1+\alpha^2}\,T^2. \tag{10}$$

In the presence of this MW field the magnetization precesses around the equilibrium position with a constant angle. This critical field represents a lower limit. Indeed, if the injected power is smaller than $p_i^{\rm crit}(\tau)$, the magnetization goes back to the initial equilibrium position.

#### *2. MW field minimizing the total injected energy: Optimal field*

In order to minimize the total injected energy we have to make a few preliminary assumptions concerning the shape of the MW field. Considering the result of the previous section we limit our search to the family of MW fields defined by

$$h_m(\tau) = \beta_m T, \quad h_u(\tau) = \beta_u T, \quad h_v(\tau) = \beta_v T,$$

where $\beta_m$, $\beta_u$, and $\beta_v$ are constant parameters. In the presence of such a MW field the energy variation reads

$$\frac{d\mathcal{E}}{d\tau} = \frac{-\alpha - \beta_u + \alpha\beta_v}{1+\alpha^2}\,T^2 - \frac{dh_m(\tau)}{d\tau}. \tag{11}$$

The total energy injected to the system can be defined as $E = \int_{\tau_i}^{\tau_f} \mathbf{h}^2(\tau) dt$. Therefore,

$$E = \int_{\tau_i}^{\tau_f} \left(\beta_m^2 + \beta_u^2 + \beta_v^2\right) T^2 d\tau = \int_{\tau_i}^{\tau f} \left(\beta_m^2 + \beta_u^2 + \beta_v^2\right) \left[\frac{1+\alpha^2}{-\alpha - \beta_u + \alpha\beta_v} \left(\frac{d\mathcal{E}}{d\tau} + \frac{dh_m(\tau)}{d\tau}\right)\right] d\tau$$
$$= \frac{(1+\alpha^2)\left(\beta_m^2 + \beta_u^2 + \beta_v^2\right)}{-\alpha - \beta_u + \alpha\beta_v} [\mathcal{E}(\tau_f) - \mathcal{E}(\tau_i) + h_m(\tau_f) - h_m(\tau_i)]. \quad (12)$$

Hence, the energy is minimal if $\beta_m = 0$, $\beta_u = -2\alpha/\left(1+\alpha^2\right)$, and $\beta_v = 2\alpha^2/\left(1+\alpha^2\right)$. Consequently, the optimal MW field is

$$\mathbf{h}^{\text{opt}}(\tau) = \frac{2\alpha}{1+\alpha^2} [-\mathbf{T} + \alpha \mathbf{m} \times \mathbf{T}] = 2\mathbf{h}^{\text{crit}}(\tau). \quad (13)$$

The optimal field is twice the critical field determined previously, see Eq. (9). It is orthogonal to the magnetization at any time and its magnitude reads

$$\|\mathbf{h}^{\text{opt}}(\tau)\| = \frac{2\alpha}{\sqrt{1+\alpha^2}} T. \quad (14)$$

The total injected energy is then

$$E = 4\alpha [\mathcal{E}(\tau_f) - \mathcal{E}(\tau_i)]. \quad (15)$$

According to these results, both the optimal field magnitude and the total injected energy increase with damping. This confirms the fact that the MW field must compensate for the effects of damping so as to induce switching.

#### 3. *Trajectory of the magnetization in the presence of the optimal MW field*

In order to check whether the optimal MW field obtained in the previous section induces switching of the magnetization as required, we now investigate the time trajectory of the magnetization. In the presence of this field, Eqs. (5) and (6), respectively, become

$$(1+\alpha^2)\frac{d\mathbf{m}}{d\tau} = -\mathbf{T} + \alpha \mathbf{m} \times \mathbf{T}, \quad (16)$$

$$\frac{d\mathcal{E}}{d\tau} = \frac{\alpha}{1+\alpha^2} T^2. \quad (17)$$

The first equation is similar to the Landau-Lifshitz-Gilbert equation but with a negative damping parameter: it describes an amplified precession. The precession frequency is equal to the proper frequency of the magnetization. At any time the MW field is proportional to the derivative of the magnetization: $\mathbf{h}^{\text{opt}}(\tau) = 2\alpha d\mathbf{m}/d\tau$. This is in agreement with the results of Sun and Wang.[7]

At the minima and saddle points the effective field $\mathbf{h}_{\text{eff}}$ is parallel to the magnetization so that $\mathbf{T} = \mathbf{0}$. Therefore, both the derivative of the magnetization and the MW field vanish. Consequently, the optimal MW field can only induce the motion of the magnetization from an initial state, $\mathbf{m}_i$, close to an energy minimum, to a final state, $\mathbf{m}_f$, close to a saddle point. A small amount of energy must thus be added (i) before the MW field pulse, to drag the magnetization away from the minimum, and (ii) after the pulse, to cross the saddle point. The nature of this additional energy will be further discussed later on. Beyond the saddle point, the damping takes up to lead the magnetization down to the second energy minimum. If the energy landscape is complex with several barriers, successive pulses might then be necessary to induce switching.

At both the initial and the final states the MW field is close to zero. The difference $\mathcal{E}(\tau_f) - \mathcal{E}(\tau_i)$ is thus close to the static energy barrier between the saddle point and the initial state $\triangle\mathcal{E}_0 \equiv \mathcal{E}_0(\tau_f) - \mathcal{E}_0(\tau_i)$ and Eq. (15) becomes

$$E = 4\alpha \triangle\mathcal{E}_0. \quad (18)$$

The total injected energy is therefore proportional to the energy barrier to be overcome. Hence, if the static field is close to the switching field, a very weak MW field can induce switching.

### C. Uniaxial anisotropy and longitudinal static field

In this section we study the trajectory of the magnetization in the presence of the optimal MW field for a nanoparticle with uniaxial anisotropy and a longitudinal static field.

We consider a nanomagnet with uniaxial anisotropy with easy axis in the $z$ direction. The anisotropy energy density is then $\mathcal{E}_{\text{an}}(m_z) = -m_z^2/2$. The static field is applied in the $(-z)$ direction with a magnitude $0 \leqslant h_0 < 1$. The magnetization is initially close to the metastable minimum and its $z$ component is thus $m_0 \equiv m_z(\tau_i = 0) \approx 1$. The static energy of the system is

$$\mathcal{E}_0(m_z) = -\frac{m_z^2}{2} + h_0 m_z. \quad (19)$$

The saddle point then corresponds to $m_z = h_0$, so the static energy barrier between the latter and the initial metastable state is $\triangle\mathcal{E}_0 = (1-h_0)^2/2$. For this system, the effective field reads $\mathbf{h}_{\text{eff}} = -h_0 + m_z \mathbf{e}_z$. Projecting Eq. (16) onto the $z$ axis then yields

$$\frac{dm_z}{d\tau} = \frac{\alpha}{1+\alpha^2}(\mathbf{m} \times \mathbf{T}) \cdot \mathbf{e}_z$$
$$= -\frac{\alpha}{1+\alpha^2}(-h_0 + m_z)\left(1 - m_z^2\right). \quad (20)$$

In order to simplify the expressions we introduce the integral

$$I(m_z) = \int_0^{m_z} \frac{-du}{(-h_0+u)(1-u^2)}$$
$$= \frac{1}{2(1-x^2)} \ln\left[\frac{(1+m_z)^{1-h_0}(1-m_z)^{1+h_0}}{(-h_0+m_z)^2}\right] + C^{te}. \quad (21)$$

Solving Eq. (20) with the initial condition $m_z(t=0) = m_0$ leads to the equation

$$I(m_z) - I(m_0) = \frac{\alpha}{1+\alpha^2} \tau. \quad (22)$$

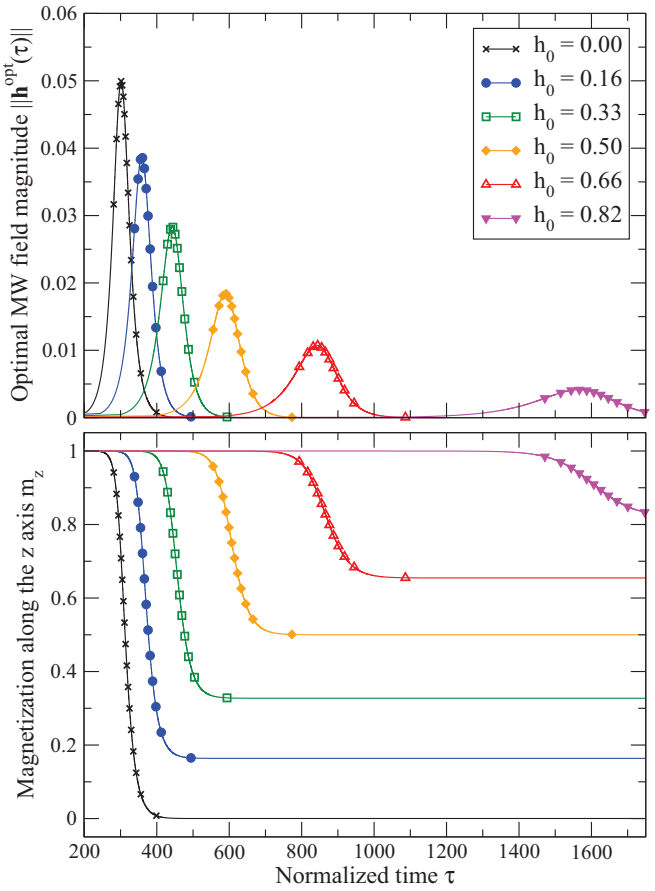


FIG. 1. (Color online) Optimal MW field intensity $\|\mathbf{h}^{opt}(\tau)\|$ (upper panel) and trajectory of the magnetization $m_z(\tau)$ (lower panel) for a longitudinal static field with magnitude $h_0$. Parameters: $\alpha = 0.05$ and $m_0 = 0.99998$.

This equation can be analytically solved for $m_z$ only if $h_0 = 0$ (no static field). Otherwise, the evolution of $m_z$ with time can be obtained numerically (see Fig. 1). As predicted previously, for long times the magnetization goes towards to the saddle point but never reaches it since $I(m_z)$ diverges for $m_z = h_0$.

From Eq. (14) we can express the optimal MW field intensity in terms of $m_z$ as follows:

$$\|\mathbf{h}^{opt}(m_z)\| = \frac{2\alpha}{\sqrt{1+\alpha^2}}(-h_0 + m_z)\sqrt{1-m_z^2}. \quad (23)$$

The time evolution of the MW field intensity is plotted in Fig. 1. We note that the pulses follow neither a Gaussian nor a Lorentzian function. The peak intensity is reached for $m_z = \frac{1}{4}(h_0 + \sqrt{8+h_0^2})$ and is given by

$$h_{max}^{opt} = \frac{\alpha}{2\sqrt{1+\alpha^2}}\left(-3h_0 + \sqrt{8+h_0^2}\right) \times \sqrt{1 - \frac{\left(h_0 + \sqrt{8+h_0^2}\right)^2}{16}}. \quad (24)$$

From this, we can see that the peak intensity $h_{max}^{opt}$ decreases with $h_0$ (see Fig. 2). Indeed, for higher magnitudes of the static field, the energy barrier $\Delta\mathcal{E}_0$ between the metastable state and the saddle point is lower, so that a lower energy is needed to reach the saddle point. Since $0 \leqslant h_0 < 1$ the peak intensity is limited as follows:

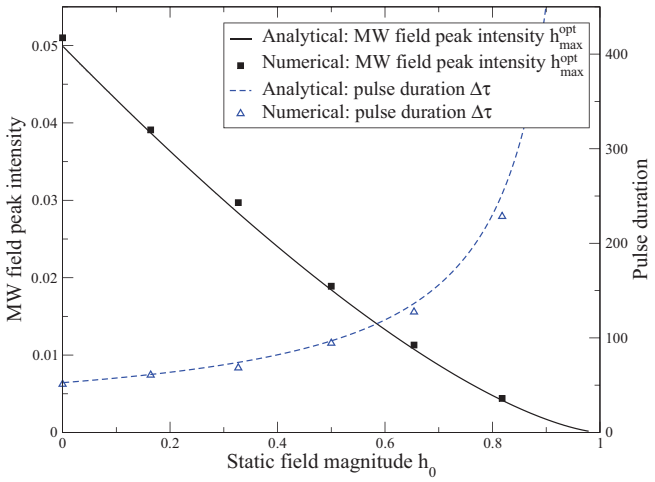


FIG. 2. (Color online) Maximal peak intensity and peak duration of the optimal MW field for varying magnitude of the static field $h_0$.

$$h_{max}^{opt} < \frac{\sqrt{2}\alpha}{\sqrt{1+\alpha^2}}. \quad (25)$$

Hence, for low values of the damping parameter $\alpha$, the intensity of the optimal MW field is small. This fully confirms the results of our numerical study.[19] Using Eqs. (21) and (23), we can also obtain analytically the pulse duration $\Delta\tau$, defined as the full width at half maximum,

$$\Delta\tau = \frac{1+\alpha^2}{\alpha} g(h_0), \quad (26)$$

where $g(h_0)$ is a cumbersome function of $h_0$. This characteristic time increases with $h_0$ (see Fig. 2). For high values of $h_0$, the switching will thus require a very low field but a very long time, as can be seen in Fig. 1. Moreover, the characteristic time decreases with damping.

The area below the curves $\|\mathbf{h}^{opt}(\tau)\|$ is

$$\begin{aligned} A &= \int_{t=0}^{t=\infty} \|\mathbf{h}^{opt}(\tau)\| d\tau = \int_{m_z=m_0}^{m_z=h_0} \|\mathbf{h}^{opt}(m_z)\| \frac{d\tau}{dm_z} dm_z \\ &= 2\sqrt{1+\alpha^2}\left[\arccos(h_0) - \arccos(m_0)\right] \\ &= 2\sqrt{1+\alpha^2}(\theta_f - \theta_i), \end{aligned} \quad (27)$$

where $\theta_i$ and $\theta_f$ are the polar angles of the magnetization at the initial state and saddle point, respectively. This area is thus proportional to the "angular distance" that the magnetization must cross to reach the saddle point. For increasing values of the static field magnitude $h_0$, this area decreases since the saddle point comes closer to the initial state.

The $z$ component of $\mathbf{h}^{opt}$, given by Eq. (13), is

$$h_z^{opt}(m_z) = -\frac{2\alpha^2}{1+\alpha^2}(-h_0 + m_z)\left(1 - m_z^2\right). \quad (28)$$

From Eq. (23) we can see that the ratio $|h_z^{opt}(m_z)|/\|\mathbf{h}^{opt}(m_z)\|$ is $\frac{\alpha}{\sqrt{1+\alpha^2}}\sqrt{(1-m_z^2)}$, whose upper limit is $\frac{\alpha}{\sqrt{1+\alpha^2}}$. Consequently, for small values of the damping parameter $\alpha$, the component of the time-dependent field along

the anisotropy easy axis can be neglected and the optimal field lies in the $xy$ plane.

We now define the precession phase of the magnetization as $\varphi(\tau) = \arctan\left[m_y(\tau)/m_x(\tau)\right]$. Projecting Eq. (16) on the $x$ and $y$ axes leads to the relation

$$\omega(\tau) = \frac{d\varphi}{d\tau} = \frac{\|\mathbf{h}_{\text{eff}}\|}{1+\alpha^2} = \frac{-h_0 + m_z(\tau)}{1+\alpha^2}. \tag{29}$$

This precession frequency is equal to the proper frequency of the magnetization, obtained by solving Eq. (3) in the absence of a MW field. At the initial state, the precession frequency is close to the ferromagnetic resonance (FMR) frequency $\omega_{\text{FMR}} = (1-h_0)/(1+\alpha^2)$. It then decreases towards zero, following the curvature of the energy well.

For small values of $\alpha$, since the optimal field lies in the $xy$ plane as shown previously, its phase can be defined by $\tilde{\varphi}(t) = \arctan[h_y^{\text{opt}}(t)/h_x^{\text{opt}}(t)]$. It can be shown that

$$\tan\tilde{\varphi}(\tau) = \frac{m_x(\tau) + \alpha m_y(\tau)\, m_z(\tau)}{-m_y(\tau) + \alpha m_x(\tau)\, m_z(\tau)} \approx -\frac{m_x(\tau)}{m_y(\tau)} = \cot\varphi(\tau). \tag{30}$$

This implies that the time-dependent field and the magnetization are synchronized with $\tilde{\varphi}(\tau) \approx \varphi(\tau) + \pi/2$. Hence, the frequency of the time-dependent field is equal to the proper precession frequency of the magnetization.

Finally, using Eqs. (20) and (23), the total injected energy can be computed. As shown previously in Eq. (18), it is proportional to the damping parameter and to the energy barrier $\triangle\mathcal{E}_0$:

$$E = \int_0^{+\infty} \|\mathbf{h}^{\text{opt}}(\tau)\|^2 d\tau = 2\alpha\,(h_0 - 1)^2 = 4\alpha\triangle\mathcal{E}_0. \tag{31}$$

## III. COMPARISON WITH THE NUMERICAL RESULTS

As mentioned earlier, in Ref. 19 we developed a numerical method based on the theory of optimal control to determine the shape of the optimal MW field. It renders an exact solution for the MW field that triggers the switching of a nanomagnet with a given anisotropy and applied field. The method consists of minimizing the cost functional

$$\mathcal{F}[\mathbf{m}(\tau),\mathbf{h}(\tau)] = \frac{1}{2}\|\mathbf{m}(\tau_f) - \mathbf{m}_f\|^2 + \frac{\eta}{2}\int_0^{\tau_f} d\tau\, \mathbf{h}^2(\tau)$$

along the trajectory given by the Landau-Lifshitz-Gilbert equation, Eq. (3), where $\mathbf{m}_f$ is the target magnetization (stable minimum), $\mathbf{m}(\tau_f)$ is the magnetization reached at time $\tau_f$, and $\eta$ is a numerical control parameter. The numerical problem is then solved using the modified conjugate gradient technique supplemented by a Metropolis algorithm.

In Ref. 19 we restricted the MW field along a polarization axis to comply with the experimental setup. In the present study, for a better comparison with the analytical results, the MW field is allowed to move in three dimensions during the optimization.

Our model system is a particle with uniaxial anisotropy along the $z$ axis. Unless otherwise specified, the numerical parameters used in the current study are as follows: initial normalized time $\tau_i = 0$; final normalized time $\tau_f = 800$ (corresponding to a few ns in real time); number of points $N = 15\,000$, so the sampling time $(\tau_f - \tau_i)/(N-1)$ is about 0.05; damping parameter $\alpha = 0.05$; and control parameter $\eta = 0.01$.

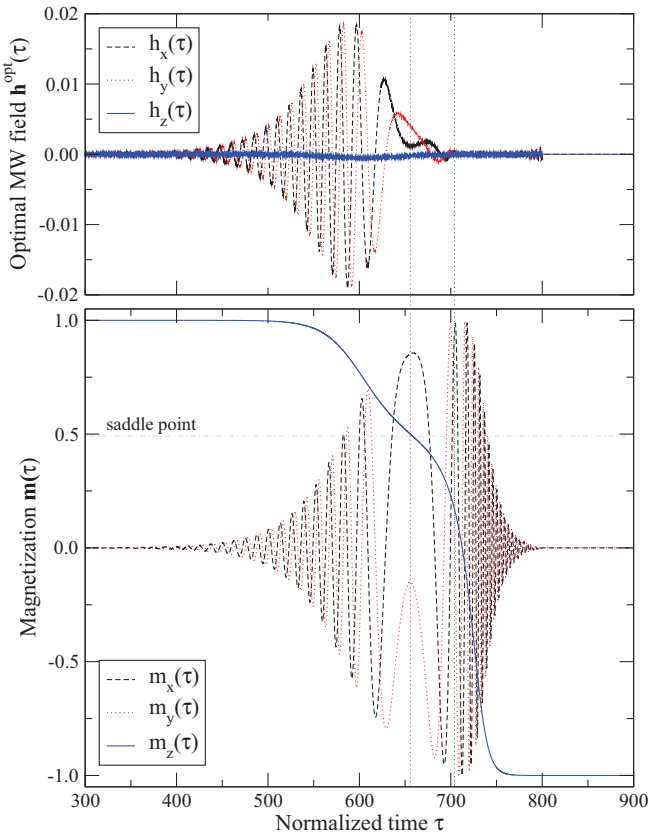


FIG. 3. (Color online) Numerical results for the reference calculation: optimal MW field (upper panel) and magnetization time trajectory (lower panel). The purple and green dotted vertical lines, respectively, indicate the crossing of the saddle point and the end of the microwave pulse.

### A. Reference calculation

A first numerical optimization was carried out for a static field with magnitude $h_0 = 0.5$ applied in the $(-z)$ direction. The results are in good agreement with the analytical calculations of Sec. II. As can be seen in Fig. 3, the optimal MW field is modulated in both amplitude and frequency. It is mainly in the $xy$ plane and its magnitude is small (less than 0.03, corresponding to a few mT in the real field) as expected since the damping parameter is small. The pulse starts at about $\tau = 350$ and progressively drives the magnetization away from the initial equilibrium position. The saddle point is reached at about $\tau = 650$ (purple dotted line) but the MW field pulse continues until $\tau = 700$ (green dotted line), which allows the magnetization to cross the saddle point. Next, the damping takes up to lead the magnetization to the more stable energy minimum, which is reached at about $\tau = 800$.

Figure 4 shows that the MW field intensity obtained numerically is in good agreement with the analytical result in Eq. (23). From $\tau \approx 570$, the MW field intensity is slightly higher numerically, which induces $m_z$ to decrease faster and the magnetization to finally cross the saddle point. The total

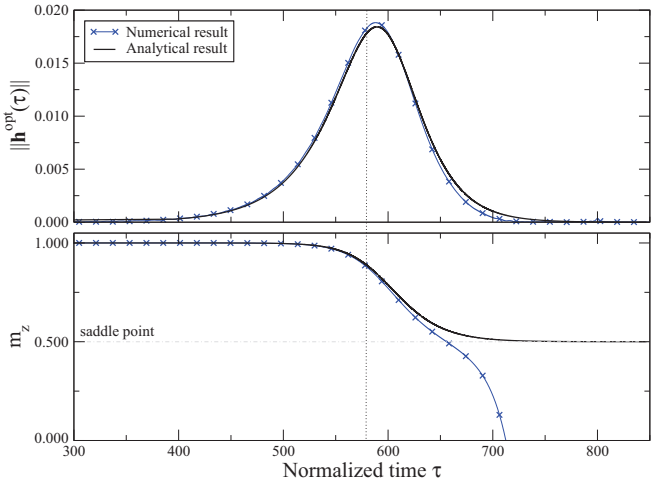


FIG. 4. (Color online) Comparison between the analytical and numerical results for the reference calculation: optimal MW field magnitude $\|\mathbf{h}^{opt}\|$(higher panel) and $z$ component of the magnetization (lower panel).

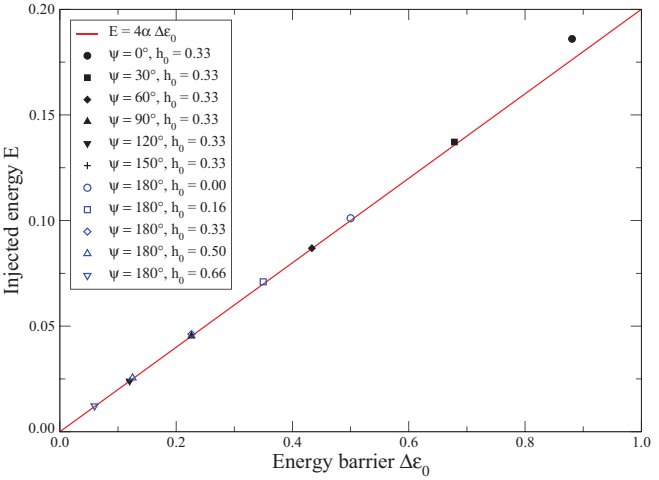


FIG. 6. (Color online) Total injected energy $E$ with respect to the static energy barrier $\triangle\mathcal{E}_0$ for varying magnitude and orientation of the static field $\mathbf{h}_0$. $\psi$ is the angle between the $z$ axis (anisotropy axis) and the static field.

injected energy obtained numerically, $E^{num} = \int_{\tau_i}^{\tau_f} \mathbf{h}^2(\tau)dt \approx 0.025\,48$, is slightly higher than the value predicted analytically, $E^{an} = 4\alpha\,\triangle\mathcal{E}_0 = 0.025\,00$. This confirms that the optimal MW field determined analytically represents a lower boundary and that a small additional energy must be injected to achieve switching, as noticed previously. Nevertheless, the discrepancy between the numerical and analytical MW fields is very small, which corroborates the relevance of the analytical model.

Figure 5 confirms that the magnetization precession and the MW field are synchronized, the initial frequency being close to the FMR frequency. The time evolution of the frequency is similar to the evolution of $m_z$ (Fig. 4), since both values are related by Eq. (29). Consequently, after $\tau \approx 570$ the numerical frequency is lower than the analytical frequency.

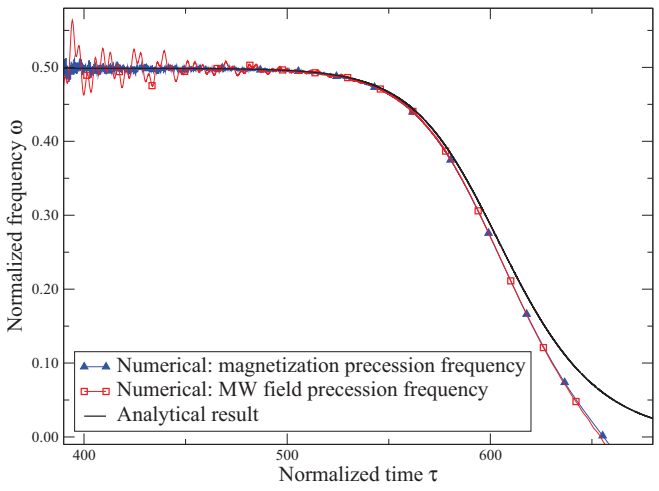


FIG. 5. (Color online) Comparison between the analytical and numerical results for the reference calculation: precession frequencies of the magnetization and MW field.

### B. Effect of the static field magnitude and direction

The MW field $\mathbf{h}(\tau)$ has been optimized numerically for several magnitudes and orientations of the static field $\mathbf{h}_0$. For each configuration, the energy barrier $\triangle\mathcal{E}_0$ and the total injected energy $E = \int_{\tau_i}^{\tau_f} \|\mathbf{h}^{opt}(\tau)\|^2 d\tau$ have been computed numerically and are reported in Fig. 6. As shown in Eq. (18), the injected energy is found to be proportional to the energy barrier and to $4\alpha$.

In the case of a static field applied along $(-z)$, the shape of the pulse can be directly compared with the analytical results of Sec. II C (see Fig. 2) . The numerical and analytical results are in good agreement. As predicted analytically, the maximal peak intensity $h_{max}^{opt}$ decreases and the pulse duration $\triangle\tau$ increases rapidly when the magnitude of the static field $h_0$ increases.

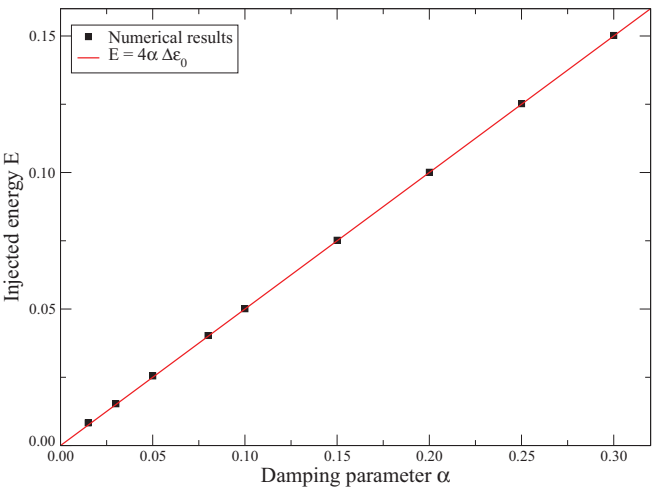


FIG. 7. (Color online) Total injected energy $E$ with respect to the damping parameter $\alpha$.

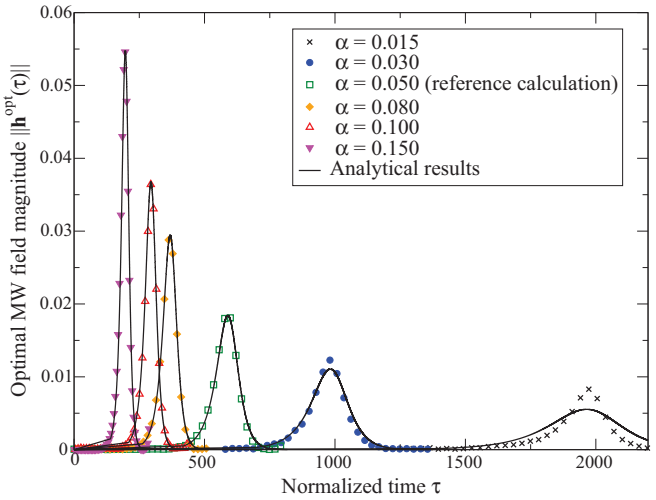


FIG. 8. (Color online) Optimal MW field pulse for several values of the damping parameter $\alpha$. For $\alpha = 0.015$, the final time has been increased ($\tau_f = 1600$) without changing the sampling time.

### C. Effect of damping

As predicted by Eqs. (18) and (31), for a given static energy barrier, $\triangle\mathcal{E}_0$, the injected energy is proportional to the damping parameter $\alpha$. This has been checked numerically by varying the damping parameter from 0.015 to 0.30 (Fig. 7). In these calculations, the static field $\mathbf{h}_0$ is applied in the $(-z)$ direction with the magnitude $h_0 = 0.5$.

Figure 8 shows that for low values of $\alpha$, the pulses' heights decrease but their durations increase, in agreement with Eqs. (24) and (26). For an undamped system, the switching should thus be infinitely long, so our analytical and numerical methods are not adapted to describe such a system.

As can be observed, for very low values of the damping parameter $\alpha$, a discrepancy between the analytical calculations and the numerical optimization is observed. Indeed, since the optimal peak duration becomes very long, the number of numerical points $N$ must be increased, so the conjugate gradient algorithm becomes less efficient. However, as can be seen in Fig. 7, this discrepancy has a negligible effect on the injected energy.

## IV. CONCLUSION

We analytically determined the optimal microwave field that allows for the switching of the magnetization of a monodomain nanoparticle with uniaxial anisotropy while minimizing the injected energy. This study provides a clear interpretation of the results obtained numerically using the optimal control theory,[19] especially the simple dependence of the pulse on the damping parameter.

Our results confirm that the optimal MW field is modulated in both amplitude and frequency, since it is directly proportional to the derivative of the magnetization. It drives the magnetization from an initial state close to the initial minimum to a final state close to a saddle point. The time trajectory can then be described as an amplified precession.

In order to cross the saddle point, a small additional energy must be injected into the system. Our numerical results show that this energy can be added by slightly increasing the MW field intensity. In reality any source of noise, such as thermal fluctuations, may suffice to induce the saddle point crossing. Subsequently, the damping induces the relaxation to the final state. We find that the injected energy is proportional to the damping parameter and to the energy barrier between the initial state and the saddle point. For typical values of the damping parameter ($\alpha < 1$), a weak MW field of a few millitesla is thus sufficient to induce switching.

For a nanomagnet with uniaxial anisotropy placed in a longitudinal static field, the shape of the MW field pulse has been obtained analytically. We have shown that the optimal MW field pulse becomes lower but more spread when the damping decreases.

In the case of more complex energy landscapes (with biaxial or cubic anisotropies) the switching is likely to be triggered by a succession of MW field pulses. This hypothesis will be later tested numerically. This study could then be extended to small nanomagnets where surface effects cannot be neglected using the effective one-spin model (EOSP).[21–23] Moreover, the influence of temperature on the optimization could be investigated numerically using the Langevin approach which introduces the temperature dependence through an additional stochastic field.[24,25] In particular, we intend to investigate the conditions under which the thermal fluctuations can favor the switching by assisting the magnetization in crossing the saddle point.

The optimal MW fields that we have found have an amplitude and a frequency which vary slowly and can be reproduced experimentally using a function generator. Consequently, our theoretical results could be used to probe the damping parameter and to assess the role of surface effects in real nanoparticles. The dependence of the MW field on the energy landscape might be used to address directly a given nanoparticle in a polydisperse assembly.

## ACKNOWLEDGMENTS

We are grateful to our collaborators E. Bonet, C. Thirion (Institut Néel, Grenoble, France), and V. Dupuis (LPMCN, Lyon, France) for instructive discussions on the microwave-assisted switching of isolated nanoclusters. This work has been partly funded by the collaborative program PNANO ANR-08-P147-36 of the French Ministry.

[1]T. Thomson, L. Abelmann, and H. Groenland, in *Magnetic Nanostructures in Modern Technology*, edited by B. Azzerboni, G. Asti, L. Pareti, and M. Ghidini (Springer, Dordrecht, The Netherlands, 2008), pp. 237–306.

[2]C. Thirion, W. Wernsdorfer, and D. Mailly, Nat. Mater. **2**, 524 (2003).

[3]G. Bertotti, C. Serpico, and I. D. Mayergoyz, Phys. Rev. Lett. **86**, 724 (2001).

[4]S. I. Denisov, T. V. Lyutyy, and P. Hänggi, Phys. Rev. Lett. **97**, 227202 (2006).
[5]G. Bertotti, I. D. Mayergoyz, and C. Serpico, *Nonlinear Magnetization Dynamics in Nanosystems* (Elsevier, Oxford, UK, 2009).
[6]Z. Z. Sun and X. R. Wang, Phys. Rev. B **74**, 132401 (2006).
[7]Z. Z. Sun and X. R. Wang, Phys. Rev. B **73**, 092416 (2006).
[8]S. Okamoto, N. Kikuchi, and O. Kitakami, Appl. Phys. Lett. **93**, 102506 (2008).
[9]G. Bertotti, I. D. Mayergoyz, C. Serpico, M. D'Aquino, and R. Bonin, J. Appl. Phys. **105**, 07B712 (2009).
[10]T. V. Lyutyy, A. Y. Polyakov, A. V. Rot-Serov, and C. Binns, J. Phys.: Condens. Matter **21**, 396002 (2009).
[11]K. Rivkin and J. B. Ketterson, Appl. Phys. Lett. **89**, 252507 (2006).
[12]G. Woltersdorf and C. H. Back, Phys. Rev. Lett. **99**, 227207 (2007).
[13]M. Laval, J. J. Bonnefois, J. F. Bobo, F. Isaac, and F. Boust, J. Appl. Phys. **105**, 073912 (2009).
[14]S. Okamoto, N. Kikuchi, and O. Kitakami, Appl. Phys. Lett. **93**, 142501 (2008).
[15]Z. Wang and W. Mingzhong, J. Appl. Phys. **105**, 093903 (2009).
[16]L. Cai, D. A. Garanin, and E. M. Chudnovsky, Phys. Rev. B **87**, 024418 (2013).
[17]B. Meerson and L. Friedland, Phys. Rev. A **41**, 5233 (1990).
[18]M. Jewariya, M. Nagai, and K. Tanaka, Phys. Rev. Lett. **105**, 203003 (2010).
[19]N. Barros, M. Rassam, H. Jirari, and H. Kachkachi, Phys. Rev. B **83**, 144418 (2011).
[20]A. Sukhov and J. Berakdar, Phys. Rev. B **79**, 134433 (2009).
[21]D. A. Garanin and H. Kachkachi, Phys. Rev. Lett. **90**, 065504 (2003).
[22]H. Kachkachi and E. Bonet, Phys. Rev. B **73**, 224402 (2006).
[23]R. Yanes, O. Chubykalo-Fesenko, H. Kachkachi, D. A. Garanin, R. Evans, and R. W. Chantrell, Phys. Rev. B **76**, 064416 (2007).
[24]W. F. Brown, Phys. Rev. **130**, 1677 (1963).
[25]C. Ragusa, C. Serpico, M. Repetto, M. d'Aquino, B. Xie, and G. Bertotti, J. Appl. Phys. **103**, 07B119 (2008).